ELSEVIER

Journal of Materials Processing Technology 185 (2007) 106–112

Journal of Materials Processing Technology

www.elsevier.com/locate/jmatprotec

Effect of heat treatment on the diffusion coefficient of hydrogen absorption in gamma-titanium aluminide

K. Suardi, E. Hamzah *, A. Ourdjini, V.C. Venkatesh

Faculty of Mechanical Engineering, Universiti Teknologi Malaysia, Johor Bahru, Malaysia

Abstract

Intermetallic alloys based on gamma-titanium aluminide are now regarded as promising candidate materials for high temperature applications such as for aerospace, marine and automotive engine components, due to their high specific strength and modulus. Their oxidation resistance is good, especially at intermediate and high temperature; oxidation resistance can be obtained up to 800 °C. One critical area of application is in combustion engine in aerospace vehicles such as hypersonic airplanes and high-speed civil transport airplanes. This entails the use of hydrogen as a fuel component and it has been widely reported by researchers that these materials exhibit environmental embrittlement in the presence of hydrogen, hence the diffusivity of hydrogen and the effect of hydrogen to the mechanical properties of γ-titanium aluminide is significant and technologically important. A fair amount of research has been carried out to investigate the influence of hydrogen in γ-titanium aluminide. Some researchers reported that α_2 and lamellar phases had major influence on the susceptibility of hydrogen to alloys, while hydrogen is too low to penetrate the γ-phases. This research focused on the effect of different microstructures obtained from various heat treatments to the diffusion coefficient and mechanical property after hydrogen absorption. Modification of γ-titanium aluminide can be achieved by heating as-cast binary samples; Ti–45% Al up to 1200 °C (above the T_e line) and cooled in three different ways: quenched, air-cooled and furnace-cooled. All samples were then subjected to corrosion attack under cathodically charged with galvanostatic mode for 6 h. The potential variation with time was monitored from these data the values of the diffusion coefficient of hydrogen to γ-titanium aluminide. D was calculated based on Fick's second law. This result was compared with that obtained from micro-Vickers hardness profiling, which was measured at cross-section area per depth from the top surface corroded. Hydrides formed at the surface were analysed by using image analyser, scanning electron microscopes (SEM) and X-ray diffraction (XRD) equipment. The results showed that different microstructures have an effect on the diffusion coefficient and mechanical property after hydrogen absorption.

Keywords: Titanium aluminide; Diffusion coefficient; Hydride; Hydrogen attack

1. Introduction

Gamma-titanium aluminide alloys are excellent candidate materials for application in aircraft engines due to their improved high temperature properties over conventional titanium alloys [1,2]. Their oxidation resistance is good, especially at intermediate temperatures and with suitable alloying additions, good oxidation resistance can be obtained up to 800 °C [3,4]. One critical area application of titanium aluminide that expose to highly hydrogen environment at low temperature is in aerospace vehicles such as hypersonic airplanes and high-speed civil transport airplanes, this entails the use of hydrogen as a fuel omponent. Other applications are in chemical storage tank such as acid or hydrogen storage tank, chemical industry medical profession, their exposure to hydrogen is inevitable, as shown in Fig. 1 [5,6]. Consequently, a good understanding of the behaviour of these materials in the presence of hydrogen is fundamental both from scientific and technological perspectives. A fair amount of research has been carried out on the influence of hydrogen in gamma-titanium aluminides [7–9]. While it is generally acknowledged that the solubility of hydrogen is low in the γ-TiAl phase (tetragonal structure) in comparison with the α_2-Ti_3Al phase (hexagonal structure) [10,11]. Thus, the objective of the present investigation is to determine the diffusion coefficient of hydrogen in heat-treated Ti–45% Al and see whether the variation in microstructure affect the diffusivity of hydrogen. This result will be compared with calculated data based on micro-hardness experimental results.

2. Experimental

The compositions of as-cast alloy used in the present study is Ti–45 at.% Al. The alloy were cut into rectangular shape samples with dimensions 15 × 15 × 5

* Corresponding author. Tel.: +60 7 553 4855; fax: +60 7 556 6159.
E-mail address: esah@fkm.utm.my (E. Hamzah).

0924-0136/$ – see front matter © 2006 Elsevier B.V. All rights reserved.
doi:10.1016/j.jmatprotec.2006.03.141

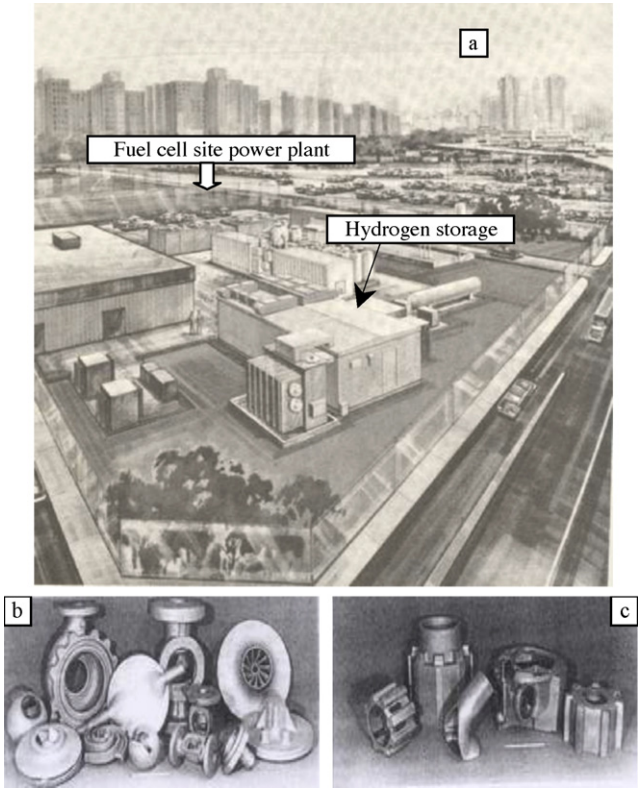

Fig. 1. Some applications of γ-titanium aluminide exposed in highly hydrogen environment: (a) rendering of a city of fuel cell site; (b) and (c) some parts used in chemical industry [5,6].

(all dimensions in mm), where only one face of the 15 × 15 area was exposed to the electrolyte.

The samples were heated up to 1200 °C, held for 30 min and then cooled at three different cooling rates, i.e. water-quenched, air-cooled and furnace-cooled. There were three samples used for the experiment as described in Table 1. This microstructure control through heat treatment is schematically depicted in Fig. 2. The specimens after heat treatment were analysed using X-ray diffraction technique.

The heat-treated samples were metallographically prepared prior to corrosion testing by cathodically charged with galvanostatic mode in 1.0 M sulfuric acid (H_2SO_4). A constant current density during the experimentation equal to 1 A/m^2 was charged to the system. To prevent the evolution of hydrogen as gas molecules, 1 g/l thiourea (NH_2CSH_2N) was added to the electrolyte as hydrogen recombination poison. During the process of electrolytic charging dissolved oxygen was eliminated by bubbling nitrogen gas through the electrolyte. Charging was carried out for 6 h. The corrosion system setup is shown in Fig. 3. Upon completion of the charging duration, the specimens were cut at cross-section area to analyse and determine the mechanical property, namely micro-hardness using micro-Vickers hardness testing machine, and to determine diffusivities using hardness property. Scanning electron microscope (SEM), EDAX and XRD were also used to examine the surface morphology of the hydrides formed.

Table 1
Samples and heat treatment processes of Ti–45% Al

Name of samples	Heat treatment; heating at 1200 °C for 30 min followed by
A	Water-quenched
B	Air-cooled
C	Furnace-cooled

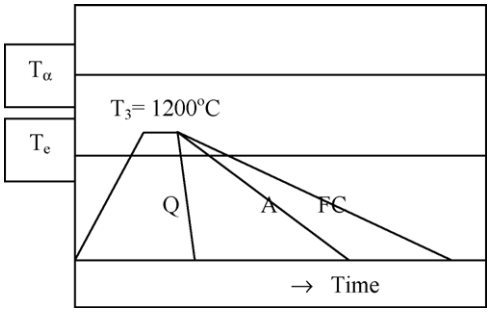

Fig. 2. Schematic temperature–time path used in heat treatment, T_α, temperature transus α phase field; T_e, temperature eutectoid; Q, quenched; A, air-cooled; and FC, furnace-cooled.

3. Results and discussion

3.1. Microstructures of Ti–45% Al before and after heat treatment

The as-cast Ti–45% Al (Fig. 4(a)) microstructure is coarse and rather inhomogeneous. It consists of columnar grains, which during solidification grow from the shell of the mold towards the center of the ingot. The prevailing lamellar constituent consisting of γ-TiAl lamellar with interspersed α_2-Ti_3Al plates. They are surrounded by interdendritic Al rich (∼54 at.% Al) γ regions [12]. The grain boundaries of Ti–45% Al are linear and the grain sizes are bigger than duplex structure, which have serrated grain boundaries [13]. Binary Ti–45% Al heated up to 1200 °C would reach α + γ through the T_e line (Fig. 4(e)), and phase transformation will take place. When heating above 1000 °C, the following transformation will occur: $\alpha_2 + \gamma \rightarrow \alpha + \gamma \rightarrow \alpha$ [12]. For quenched sample (Fig. 4(b)), after phase transformation through T_e line, the atoms in phases did not have enough time to re-arrange themselves due to fast cooling, causing the grains to become small. The grain size of lamellar vary from 70 to 200 μm. The lamellar phases formed became fragmented platelets due to fast cooling with a width of about 7 μm (Fig. 4(f)).

In air-cooled sample (Fig. 4(c)), α_2, lamellar and γ phases are formed. Unlike quenched samples the lamellar grains are bigger in air-cooled, with grain size about 160 μm. Furnace-cooled sample (Fig. 4(d)), also has α_2, γ and lamellar phases. Lamellar grains have bigger size than that of quenched and air-cooled,

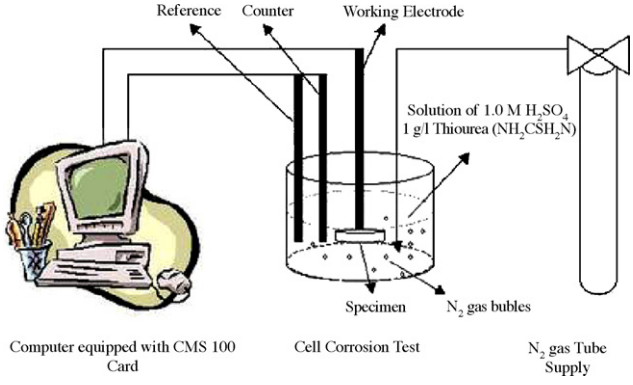

Fig. 3. Schematic diagram of corrosion system setup.

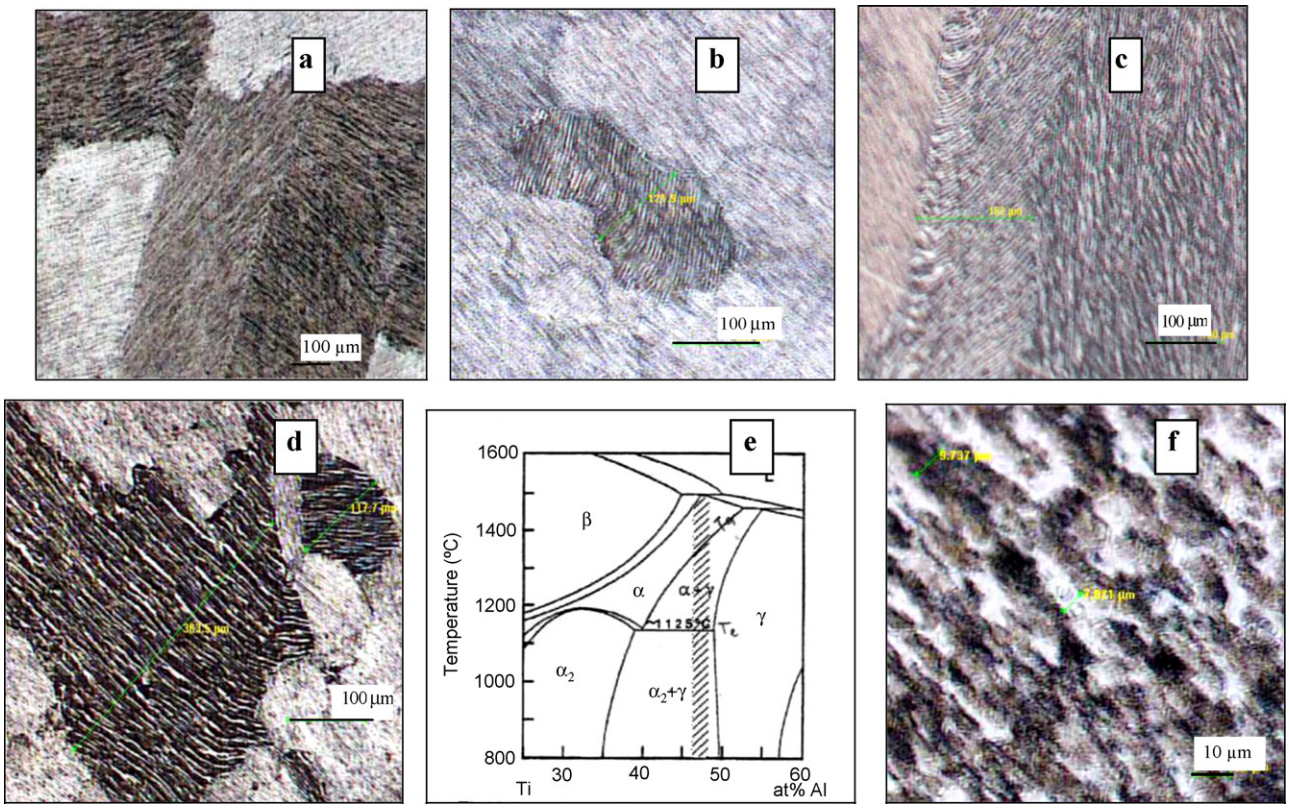

Fig. 4. (a) As-cast Ti–45% Al; heated at 1200 °C; followed (b) water-quenching; (c) air-cooling; (d) furnace-cooling; (e) central portion phase diagram of γ-TiAl; and (f) fragmented α_2 platelets in lamellae phase.

ranging from 150 to 420 μm. Also γ grains of furnace-cooled sample are bigger than that in quenched and air-cooled samples, i.e. about 150–300 μm. Slow cooling, with rate cooling approximately 10 °C/min provide enough time for phases and atoms in grains to arrange themselves to stable condition and produce bigger grains than those of quenched and air-cooled samples.

Fig. 5 shows the X-ray diffraction spectrums of Ti–45% Al heat treatment before cathodically charged in sulfuric acid. Fig. 4(a–c) show the Ti–45% Al heated up to 1200 °C and water-quenched, air-cooled, and furnace-cooled, respectively. These figures show that the intensity of α_2-phase is higher in the quenched specimen compared to the air- and furnace-cooled samples. With the lower cooling rate (furnace-cooled) α_2-phase formed is low compared to the gamma phase [14].

3.2. Determination diffusivities using electro chemical data

Electrochemical techniques have been used recently to measure the diffusion coefficient, D, using various modes [15]. In this case, the galvanostatic mode was used where a small constant current is passed through the cell for a time interval t. Thus, a constant flux of the diffusing species (in this case, hydrogen) is maintained at the electrode/electrolyte interface, $x = 0$. The voltage between the sample electrode (here, the gamma-titanium aluminide) and a reference electrode is monitored as a function of time during this current flow. The measured voltage at the cell provides a direct measure of the activity of the diffusing component, in this case hydrogen. Thus, the determination of the diffusion coefficient of hydrogen in these gamma-titanium aluminide alloys is simply a question of solving Fick's second law [16] with the appropriate boundary conditions.

$$\frac{\partial C}{\partial t} = \frac{\partial}{\partial x}\left(D\frac{\partial C}{\partial x}\right) \tag{1}$$

At the electrode/electrolyte interface, assuming steady state is reached, i.e the amount of hydrogen discharged is constant,

$$I(t) = -zFSD\left(\frac{\partial C}{\partial x}\right)_{x=0} \tag{2}$$

Assuming that the diffusion coefficient of hydrogen is approximately constant for small changes in composition of the gamma-titanium aluminide alloys, Eq. (1) becomes:

$$\frac{\partial C}{\partial t} = D\frac{\partial^2 C}{\partial x^2} \tag{3}$$

Also, since the diffusion is in the perpendicular direction and the diffusion distance is very small compared to the specimen area, one-dimensional diffusion is assumed. Under the experimental conditions mentioned above, the initial and boundary conditions are:

$$C = C_o \quad 0 \le x \le L, \quad t = 0 \tag{4}$$

$$-D\frac{\partial C}{\partial x} = \frac{I}{zFS} \quad x = 0, \quad t > 0 \tag{5}$$

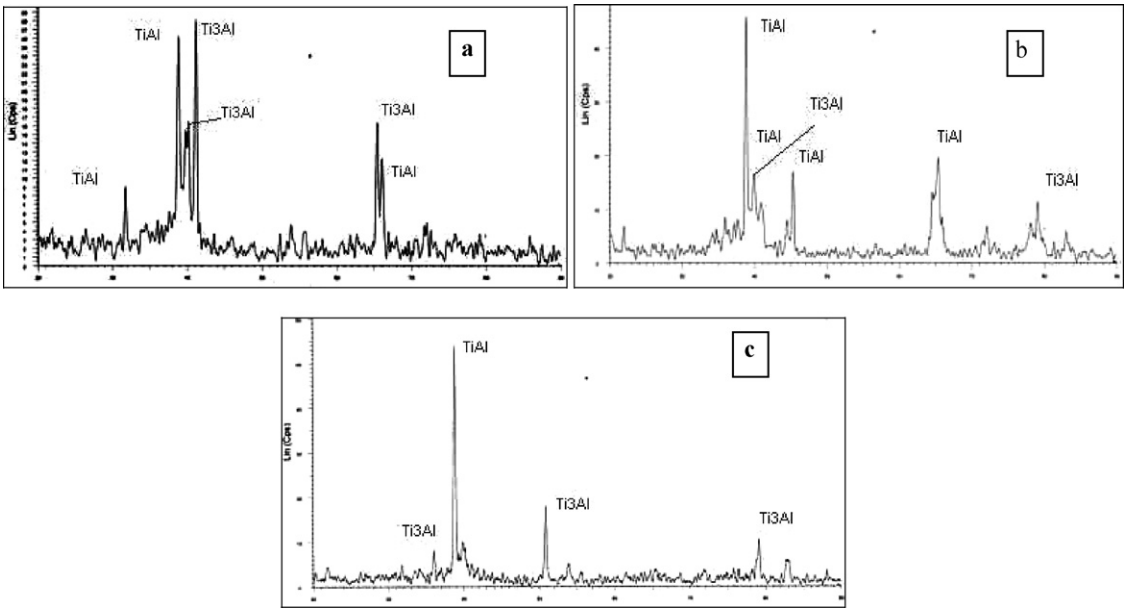

Fig. 5. X-ray diffraction analysis on heat-treated Ti–45% Al: (a)–(c) water-quenched, air-cooled, and furnace-cooled, respectively.

$$\frac{\partial C}{\partial x} = 0 \quad x = L, \qquad t \geq 0 \tag{6}$$

Here, C, z, F and S are the concentration of the diffusing species (hydrogen), charge number of the electro-active diffusing species, the Faraday constant and the sectional area common to both the electrode and electrolyte, respectively. I is the constant current in the electrolytic cell. L, which is the distance from the surface where $\partial C/\partial x = 0$, is the sample half-thickness, i.e where the hydrogen concentration approaches the base hydrogen content of the gamma-titanium aluminide base material. With the assumption of constant D for small changes in composition, Fick's second law is solved for the above boundary conditions.

The solution to Eq. (3) is in the form of an error function or infinte series [17] and for short times it is given by:

$$C_s(t) - C_o = \frac{2IV_m}{zFS(\pi D)^{1/2}} \frac{dE}{d\delta} \quad t <<< \frac{L^2}{D} \tag{7}$$

It is convenient to differentiate Eq. (7) with respect to $t^{1/2}$ and after some manipulation [12] to rewrite it as:

$$\frac{dE}{dt^{1/2}} = \frac{2IV_m}{zFS(\pi D)^{1/2}} \left(\frac{dE}{d\delta}\right) \tag{8}$$

Here, $(dE/d\delta)$ is the variation in potential of the gamma-titanium aluminide electrode with change in the hydrogen composition and V_m is the molar volume of the titanium aluminide electrode. As can be seen from Eq. (8), the quantity $(dE/d\delta)$ can be obtained from the slope of a linear plot of E versus $t^{1/2}$. At longer times and for the above boundary conditions, the solution to Fick's second law is also in the form of an infinite series. The higher order terms are neglected as an approximation and only the first two terms are differentiated with respect to t, which results in the following equation:

$$\frac{dE}{dt} = \frac{IV_m}{zFSL} \left(\frac{dE}{d\delta}\right) \quad t >>> \frac{L^2}{D} \tag{9}$$

With the assumption that $(dE/d\delta)$ is sufficiently constant, this value can be calculated approximately from the slope of the E versus t curve at long times (see Fig. 6).

For long times, since the voltage is a linear function of time (see Fig. 6), the diffusion coefficient can also be calculated from the following equation [15,17]:

$$[E_{(t)} - E_{(t=0)}]_{t=0} = \frac{ILV_m}{3zFSD} \left(\frac{dE}{d\delta}\right) \tag{10}$$

$E(t)$ is the extrapolated intercept from the linear part of the E versus t curve at $t\sqrt{0}$. $E(t\sqrt{0})$ is the net voltage after eliminating the ohmic voltage change when the current in the electrolytic cell is turned on. The results of diffusivities calculated from electrochemical data are shown in Table 2.

3.3. Determination of diffusivities using micro-hardness test

Calculations of the diffusion coefficient using measured micro-hardness values have been made for oxygen and nitrogen diffusivities in titanium-based alloys [18,19]. Although it is acknowledged that the hardness and hydrogen concentration do not strictly vary linearly with each other, approximate linearity does exist for relatively dilute concentrations of solute [8] as would be the situation in this case.

Furthermore, since it is impossible to determine the microhardness exactly at the surface, a measurement very close to the surface, which is at cross-section area per depth was taken and assume to correspond to surface concentration. In this research, this simple but effective technique was used mainly for comparison purposes.

Table 2
Values of D calculated from electrochemical methods and micro-hardness test results

Name of samples	Heat treatment; heating at 1200 °C for 30 min followed by	ΔE ($E_{(t=6)} - E_{(t=0)}$)	D calculated from Eq. (10) (cm^2/s)	Hardness values in three location: Hv_1, Hv_2, Hv_0	D calculated from micro-hardness test (cm^2/s)
A	Water-quenched	7.47	3.98×10^{-6}	220, 321, 337	1.48×10^{-6}
B	Air-cooled	0.26	0.56×10^{-6}	348, 357, 330	7.6×10^{-6}
C	Furnace-cooled	0.25	3.4×10^{-6}	306, 284, 295	0.29×10^{-6}

The variation of micro-Vickers hardness (Hv) in the subscale per depth is due to the variation of concentrations of diffusing species of the hydrogen. Assuming $(C - C_0)$ to be proportional to increase of Hv over the bulk value $(Hv - Hv_0)$ [19];

$$\frac{C - C_o}{C_s - C_o} = \frac{Hv - Hv_o}{Hv_s - Hv_o} \tag{11}$$

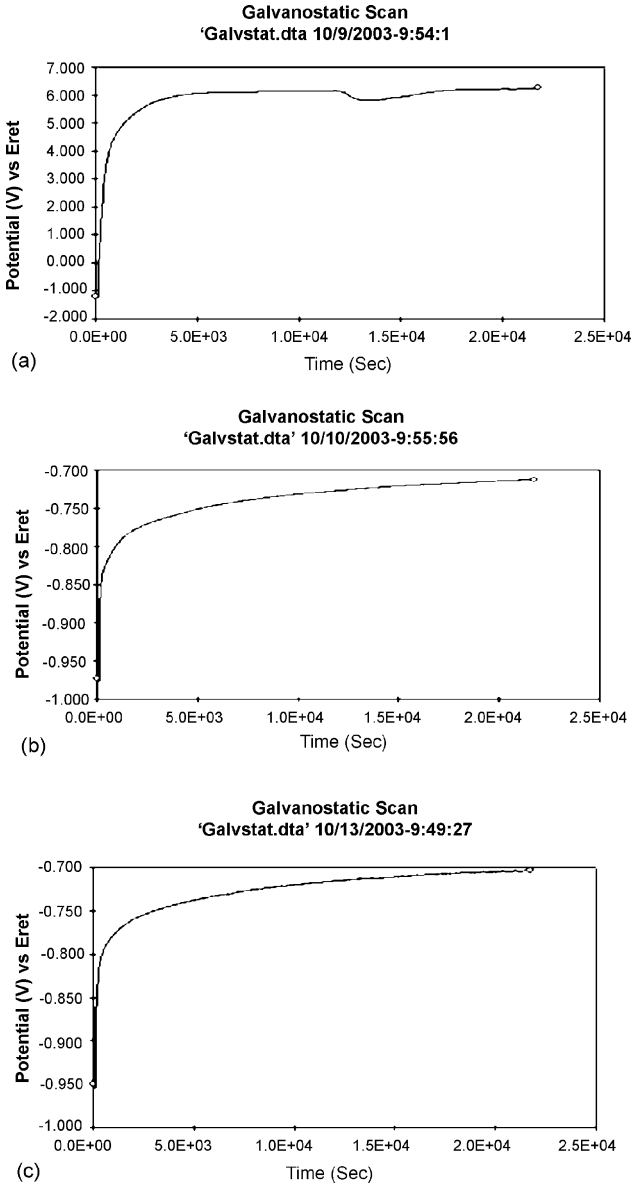

Fig. 6. Potential variation with time during hydrogen charging (a) and (b) Ti–45% Al water-quenched and air-cooled. (a)–(c) Ti–45% Al water-quenched, air-cooled, furnace-cooled, respectively.

where C is the concentration of diffusing species at a given distance. Value C_o/Hv_o and C_s/Hv_s denote bulk and surface, respectively. As the specimen surfaces were flat and the depths of diffusion field were very small compared to the thickness of samples, the problem may be treated as unsteady diffusion through a semi-infinite flat specimen. Assuming that (i) diffusion occurred through a single phase; (ii) no internal oxidation in the diffusion field; (iii) the diffusion coefficient (D in cm^2/s) was constant in the entire diffusion zone; and (iv) the surface concentration (C_s) was constant and not a function of time, Eq. (11) can be combined with the standard diffusion equation to obtain;

$$\frac{Hv - Hv_o}{Hv_s - Hv_o} = \frac{C - C_o}{C_s - C_o} = 1 - erf\left(\frac{z}{2\sqrt{Dt}}\right) = erfc\left(\frac{z}{2\sqrt{Dt}}\right) \tag{12}$$

where z is the distance from hydride interface (in cm) and t is the known exposure time (in s). It maybe noted for some experimental conditions the micro-hardness profiles exhibited either scatter or insignificant variation. Determination of diffusivity for these cases would be unreliable. In this case the assumption of constant surface concentration (C_s) in Eq. (12) may not be strictly valid as C_s may vary due to variation in the nature of growing hydride on the surface with time and Eq. (12) is not expected to be obeyed well. Therefore, the technique consisted of picking up various pairs of points on the smoothed micro-hardness versus distance curve and employing the following procedure; for two given points 1 and 2, the parameter Y_{12} could be obtain on the basis of Eq. (12) as follows [18]:

$$Y_{12} = \left(\frac{C_1 - C_o}{C_2 - C_o}\right) = \frac{erfc\,(z_1/2\sqrt{Dt})}{erfc\,(z_2/2\sqrt{Dt})} = \frac{Hv_1 - Hv_0}{Hv_2 - Hv_0} \tag{13}$$

where Hv_1 is the micro-Vickers hardness value at location z_1, Hv_2 at location z_2 and Hv_0 the bulk micro-Vickers hardness value. Since Y_{12} is a ratio, errors in the estimated values of D would partly be eliminated due to cancellation effect. This also eliminates C_s, which is an unknown. This is the rationale behind the procedure based on Eq. (13). The diffusivity (D) is the only unknown parameter in the above equation as the exposure time for each experiment is known. By using an error function, values of D were obtained, as shown at Table 2.

3.4. Diffusion coefficient analysis

The D value obtained by using electrochemical data is almost similar to those calculated from the micro-hardness

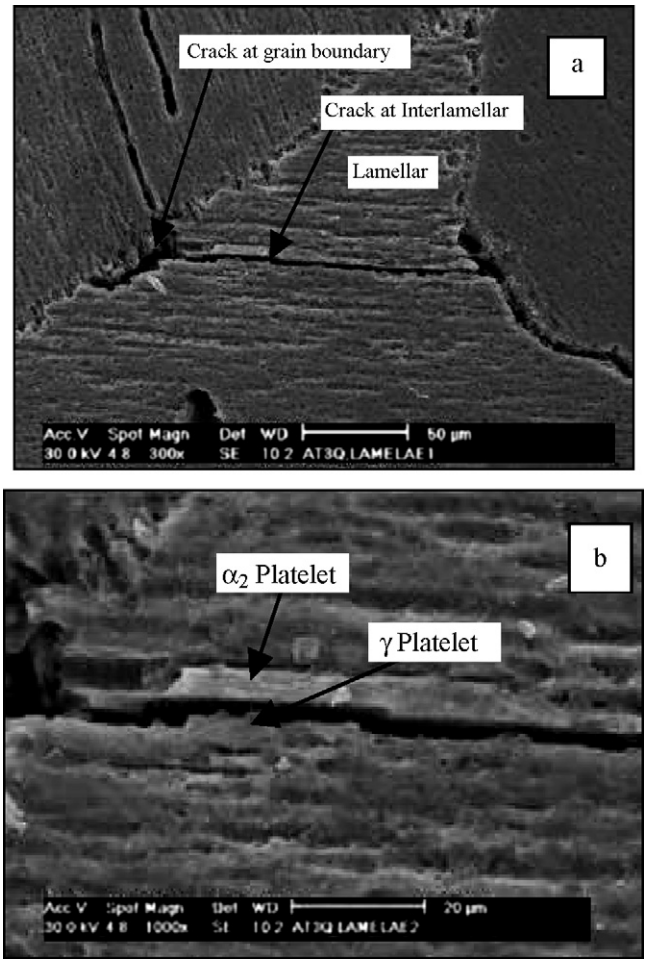

Fig. 7. Crack occur at grain boundaries and at platelets between α_2 and γ plate in lamellar phase: (a) ×300 and (b) ×1000 (continued).

result (see Table 2). However, sample A, B and C show variation by factors of 2.68, 13.5 and 11.7, respectively. Those factor values are acceptable considering the difficulties in micro-hardness measurements close to the surface. Values of D for hydrogen in commercially pure polycrystalline titanium have been recently reported from permeation experiments to be $D = 2.6 \times 10^{-10}$ cm^2/s for interstitial diffusion and $D = 9.1 \times 10^{-5}$ cm^2/s for grain boundary diffusion [20]. The value of D reported in this research is similar to the value of diffusion coefficient for grain boundary diffusion. It remains to be determined if this hydrogen diffusion in Ti–45% Al is predominantly diffusion through along grain boundary and interlamellar.

From different microstructure generated by heat treatment shown in Table 2, sample A was the worst permeated by hydrogen compared to others. It also can be explained from SEM images in Fig. 7. Hydrogen ions attack caused severe corrosion on the water-quenched Ti–45% Al sample. Water-quenched sample contains more percentage of α_2-Ti_3Al (hexagonal structure), as shown in Fig. 5(a). It is acknowledged that α_2-Ti_3Al phase absorb more hydrogen than γ-TiAl phase (tetragonal structure) [10,11].

There are many cracks at the grain boundaries and cracks at the platelets between α_2 and γ in lamellar phase occurred in the quenched sample. The present results are in good agreement with previous investigations [21,22].

Other research studies by Abe et al. and Hashi et al. [23,24] reported that hydrogen induced local amorphization at interlamellar boundaries in lamellar phase. These facts probably explain why cracks occur at the grain boundaries and at interlamellar regions.

Cracks at the grain boundaries also occur in the air-cooled sample but slightly less than those in the quenched sample. The furnace-cooled sample showed the least of cracks as shown in Fig. 8.

4. Conclusions

- The room temperature diffusion coefficient (D) of hydrogen in heat-treated gamma-titanium aluminide (Ti–45% Al) are (3.98, 0.56, 3.4) × 10^{-6} cm^2/s for water-quenched, air-cooled and furnace-cooled, respectively. Those values were compared using micro-Vickers hardness measurement, with D values are (1.48, 7.6, 0.29) × 10^{-6}, respectively.
- It is deduced that hydrogen may have diffused through the grain boundaries and interlamellar regions between alpha-2 and gamma platelets.
- It was found that variation in microstructure has an effect on the hydrogen attack with quenched sample was the worst

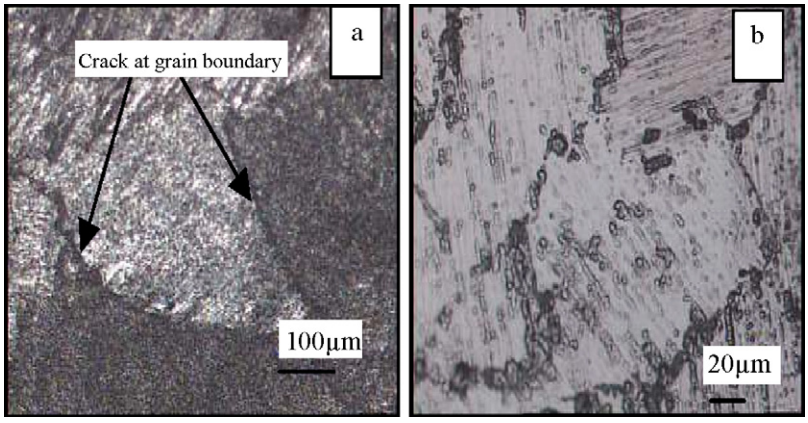

Fig. 8. Heat-treated Ti–45% Al after charged (a) air-cooled sample and (b) furnace-cooled sample.

attacked by hydrogen embrittlement compared to air-cooled and furnace-cooled samples.
- It is deduced that higher cooling rate in heat treatment of Ti–45% Al result in low resistance to hydrogen permeation to the alloy.

Acknowledgement

The authors would like to thank the Malaysian Ministry of Science, Technology and Environment for the research fund under an IRPA program (Project No. 09-02-06-0002 EA-002).

References

[1] Y.W. Kim, Microstructural evolution and mechanical properties of a forged gamma titanium aluminide alloy, JOM (1991) 1121–1122.
[2] Y.W. Kim, D.M. Dimiduk, Progress in the understanding of gamma titanium aluminides, JOM 41 (1989) 24.
[3] N. Zheng, W.J. Quadakkers, A. Gil, H. Nickel, Oxid. Metals 44 (1995) 477.
[4] H. Nickel, N. Zheng, A. Elschner, W.J. Quadakkers, Microchim. J. Acta Mater. 119 (1995) 23.
[5] W. Sha, C.J. McKinven, Experimental study of the effect of hydrogen penetration on gamma titanium aluminide and Betta 21s titanium alloys, J. Alloys Compd. 335 (2002) L16–L20.
[6] Malcolm, A. Fullenwider, Hydrogen Entry and Action in Metals, Pergamon Press, USA, p. 80, ISBN 0-08-027526-5.
[7] A. Zeilinski, Hydrogen-assisted degradation of some non-ferrous metals and alloys, J. Mater. Process. Technol. 109 (2001) 206–214.
[8] P.A. Sundaram, E. Wessel, P.J. Eunis, W.J. Quadekkers, L. Singheiser, Diffusion coeficient of hydrogen in a cast gamma titanium aluminide, J. Scrip. Mater. 41 (no. 1) (1999) 75–80.
[9] A.W. Thompson, Environmental Effect on Advances Materials, in: R.E. (Ed.), TMS-AIME, Warrendale, PA, 1988, p. 21.
[10] A. Takasaki, Y. Furuya, Hydride formation and thermal desorption spectra of hydrogen of cathodically charged single-phase gamma titanium aluminide, J. Scrip. Mater. 40 (1999) 595–599.
[11] A. Takasaki, Y. Furuya, Hydrogen evolution from chemically etched titanium aluminides, J. Alloys Compd. 243 (1996) 167–172.
[12] F. Appel, R. Wagner, In Reports: A Review Journal, Mater. Sci. Eng. R22 (1998) 187–268.
[13] S. Mitao, S. Tsuyama, K. Minakawa, Effect of microstructure on the mechanical properties and fracture of gamma-base titanium aluminide, J. Mater. Sci. Eng. A143 (1991) 51–62.
[14] E. Hamzah, K. Suardi, A. Ourdjini, K.W. Lau, Effect of heat treatment on microstructure and hardness of γ-base titanium aluminide, J. Inst. Mater. Malays. 4 (2003) 83–101.
[15] C.J. Wen, C. Ho, B.A. Boukamp, I.D. Raistrick, W. Weppner, R.A. Huggins, Int. Metall. Rev. 5 (1981) 253.
[16] Pat.L. Mangonon, The Principles of Materials Selection for Engineering Design Int. ed., Prentice Hall International. Inc, USA, 1999, ISBN 0-13-095722-4.
[17] J. Crank, The Mathematics of Diffusion, Oxford University Press, London, 1967, ISBN 0-19-853411-6, pp. 11–27.
[18] T.K. Roy, R. Balasubramaniam, A. Ghosh, Determination of oxygen and nitrogen diffusivities in titanium aluminide by subscale microhardness profiling, J. Scrip. Mater. 34 (1996) 1425.
[19] K.N. Strafford, J.M. Towell, J. Oxid. Metal. 10 (1976) 41.
[20] O.S. Abdul-Hamid, R.M. Latanison, in: A.W. Thompson, N.R. Moody (Eds.), Hydrogen Effects in Materials, TMS, Warrendale, PA, 1996, p. 205.
[21] A.M. Brass, J. Chene, Hydrogen Absortion in Titanium Aluminides Exposed to Aqueous Solution at Room Temperature, J. Mater. Sci. Eng. A 272 (1999) 269–278.
[22] K.W. Gao, M. Nakamura, Effect of hydrogen on tensile properties of Ti–49% Al alloy, J. Scrip. Mater. 143 (2000) 135–140.
[23] E. Abe, K.W. Gao, M. Nakamura, Local amorphization in hydrogen-charged two-phase TiAl alloy, J. Scrip. Mater. 42 (2000) 1113–1118.
[24] K. Hashi, K. Ishikawa, K. Suzuki, K. Aoki, Hydrogen induced amorphization in off-stoichiometric Ti_3Al, J. Scrip. Mater. 44 (2000) 2591–2595.